Numerical Simulation and Comparative Study of Aerodynamic Performance of Kline-Fogleman Modified Backward Stepped Airfoils and the NACA 4415 Airfoil

Asif Kabir[1], Mehran Islam[2*], Nusrat Jahan[3], Yeasir Mohammad Akib[4] and Most Israt Jahan Mili[5]

Abstract

This research predominantly centers on the streamlined qualities of Kline-Fogleman modified (KFm) airfoil. KFm arrangement airfoil family shows improved strength and low stalling which has made it quite popular for low weight conveying flight. Some of the major streamlined attributes like lift coefficient, drag coefficient, etc. of KFm-1, KFm-2, and KFm-3 have been explored and a correlation is made with the NACA 4415 airfoil. Spalart-Allmaras disturbance model is applied to the ANSYS Fluent commercial software. The setup is analyzed at a different angle of attack (AOA) methodologies stretching out from 0˚ to 15˚ and for a variety of Mach numbers ranging from 0.3 to 0.6. The Reynolds number was 3.18 $\times 10^5$. The purpose of this division was to reduce computational costs while utilizing CFD software. Computational assessments were coordinated to explore the streamlined presentation of the airfoil. The results highlighted that a steady and gradual increase in lift is possible by introducing the backward step. The overall aim of this assessment was to numerically inspect whether the streamlined execution of an airfoil can be improved by introducing a backward-facing step on the upper surface of the airfoil.

Keywords: Kline-Fogleman modified airfoil, NACA series, Lift force, Drag force, Computational Fluid Dynamics.

---

[1]*Department of Mechanical Engineering, Bangladesh University of Engineering and Technology (BUET), Dhaka, Bangladesh; asifkabir121@gmail.com*

[2]*Department of Naval Architecture and Offshore Engineering, Bangabandhu Sheikh Mujibur Rahman Maritime University, Dhaka, Bangladesh. mehran.naoe@bsmrmu.edu.bd*

[3]*Department of Physics, Bangabandhu Sheikh Mujibur Rahman Maritime University, Dhaka, Bangladesh. nusrat.phy@bsmrmu.edu.bd*

[4]*Department of Industrial and Production Engineering, Rajshahi University of Engineering and Technology (RUET), Rajshahi, Bangladesh. yeasir.akib@gmail.com*

[5]*Department of Oceanography & Hydrography, Bangabandhu Sheikh Mujibur Rahman Maritime University, Dhaka, Bangladesh. mili.oh@bsmrmu.edu.bd*

**Corresponding Author*

Introduction

Wings generate lift to hold the plane in the air and helps it to fly in different flight conditions through the dynamic reaction with air. The cross-sectional shape of the wing is known as an airfoil. Figure 1 shows a typical airfoil with its different components. The unique shape of the wings creates a pressure difference between the upper and lower surface of the wing which in result generates two forces, a net upward force called lift and a horizontal force called drag, in the direction of the flow. The lift can increase or decrease depending on several parameters like the angle of attack (AOA), wing area, velocity, the density of the air, or the shape of the airfoil. It is to be noted that, some of these parameters are interconnected with each other such as the angle of attack with the shape of the airfoil and efficiency of a wing with the angle of attack. The efficiency of a wing is determined by the lift to drag ratio and lift is dependent on AOA, the efficiency is indirectly related to the shape of the airfoil. There are many different types of airfoils such as symmetric, nonsymmetrical airfoils, blade twist, wedge shape airfoils, stepped, etc. and they have different use depending on their shape. For example, a double wedge shape airfoil is used for space programs because it can produce a higher Mach number in the hypersonic range (Kabir, Hossain, et al. 2019).

At the beginning of aircraft development, airfoils were designed by trial and error method without a proper system. This scenario was changed by the NACA (National Advisory Committee for Aeronautics) of the USA. They used the previously developed theories in the airfoil and boundary layer concept and systematically designed and tested a large number of airfoils in the 1930s. These designs are designated as NACA airfoils and the shape of the NACA airfoils is described using a series of digits. NACA series have a wide collection of airfoil shapes from symmetrical to nonsymmetrical. Amongst the symmetrical airfoil NACA- 0012 is one of the most popular ones with high aerodynamics efficiency (Kabir, Hasan, and Akib, 2019). But its limitations lie with the increase of angle of attack, AOA. Increasing the AOA affects both the lift and induced drag for NACA-0012 and at the AOA of 15°, the airflow above the upper surface of the airfoil gets detached (Hasan, Kabir and Akib 2019). This detachment causes the wings to lose the lift and come to a condition called stalling. On the other hand, NACA 4415 is a nonsymmetrical airfoil that has been found by (David and Jamey 2002) to reduce the flow separation shown while they were working with the oscillation of the upper surface of an airfoil.

Stalling is associated with flow separation due to the adverse pressure gradient along the flow surface. This phenomenon is undesirable as it reduces the aerodynamic performances significantly by increasing the drag, decreasing the lift, and sometimes causing vibrational failure. Regarding this problem, different flow control techniques

both in active and passive form and airfoil modifications have been implemented over the years. As an active flow control technique, the plasma actuator has been found to show good performance recently. (Hasan and & Atkinson 2020) Discussed details of the plasma actuator on the external aerodynamic flow control. Whereas, vortex generators are the most popular passive flow control technique.

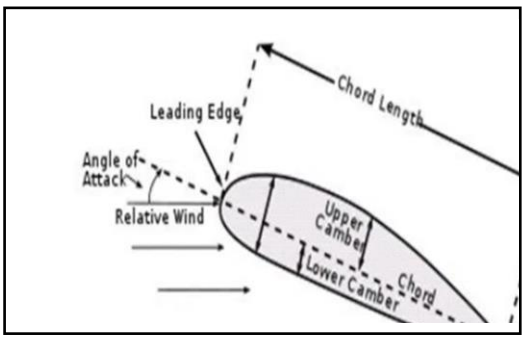

Figure 1: (a) A typical airfoil with its different component (Bandakkanavar 2015)

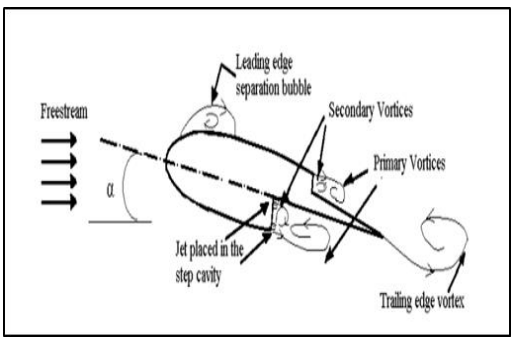

Figure 1: (b) Flow field around the upper and lower stepped airfoil (Ranganadhan 2012)

passive manner that are also commonly used in aerospace industries, such as, turbulizers, suction, and blowing mechanism, etc. Vortex generators (VGs) create a swirl in the flow that induces energy into the near-wall portion through a counter-rotating vortex to suppress the separation due to an adverse pressure gradient. Although VGs are passive, i.e. they cannot be operated under varying conditions, the main advantages of having them are low-cost structures, simplistic design, and robustness. This passive flow control technique of Vortex generations (VG) and its trapping was first used by Witherspoon (Witherspoon 1996). He showed by adding backward-facing steps in NACA-0012 the aerodynamics performance can be enhanced. Besides, NACA-0012, the idea of adding backward-facing steps was also studied using NACA-0015 by many researchers (Kabir, Chowdhury, et al. 2019). In 1975, Kasper first claimed to use the vortex generated glider called Kasper tailless glider and his research showed the possibility of an aircraft with safety, economy, stability, and STOL (Short Takeoff and landing) capability (Kasper 1975). Following his work in 1977, Kruppa showed the efficiency of the Kasper tailless glider through a wind tunnel experiment (Kruppa 1977). But the shortcoming of the Kasper glider was that it required external energy sources to gain a significant vortex lift.

The idea of this backward-facing step was further analyzed by Kline and Fogleman in 1977 who developed a series of stepped airfoils known as the KFm- series (Kline and Fogleman 1977). The benefits of Kline and Fogleman airfoil was its simple construction and the least amount of mechanical actuation being utilized. Its unique shape produces a vortex in the stepped portion of these airfoils. Figure 1(b) shows the

vortex generation for two types of KFm. When the backward-facing step is on the upper surface of the airfoil and far from the leading edge, two types of vortex named primary and secondary vortex is generated. This captured vortex allows the air to travel on the wing without creating any friction which decreases the drag and results in high efficiency. The captured vortex also sucks the airflow down to the trailing edge of the wing making the airstream less prone to separation. Thus, the airfoil becomes resistant to stalling and keeps air flowing over the control surfaces, even at high angles of attack.

Figure 2: (a) A triple KFm-2 airfoil in action (Davereap 2017)

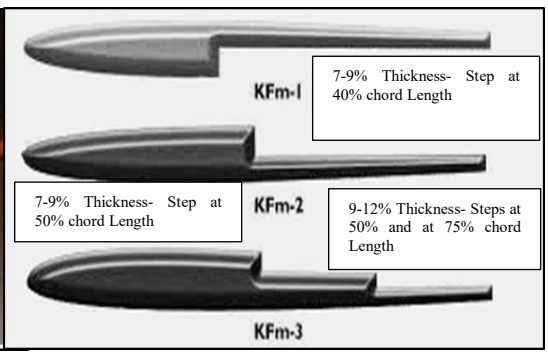

Figure 2: (b) KFm airfoil series (Davereap 2017)

The KFm series is classified depending on the position of the steps such as steps either on the bottom (KFm 1) or on the top of an airfoil (KFm 2), or both on top and bottom (KFm 4) or with two steps on the top (KFm 3) and so on. The first successful application of upper stepped KFm airfoil was found in Fertis's work. The particular airfoil had a step in 50% chord with 50% depth (Fertis 1994). His research confirmed that the KFm airfoil can have the potential design to maneuver over a long range of flight. Moreover, Boroomand presented a study on backward-facing step airfoil and its efficiency for a large Reynolds number flow (Boroomand and Hosseinverdi. 2009) concluding that symmetrical airfoil has a less long-range of flight than nonsymmetrical airfoil. There have already many studied for the nonsymmetrical airfoil.

Considering the previous literature, it is reasonable to study the efficiency of different types of KFm to find its possible application. Keeping this goal in the mind, this study was aimed to compare the aerodynamic efficiency as a function of AOA for 3 different KFm- airfoil namely KFm-1, KFm-2, and KFm-3, and correlate the most efficient one of the three with a traditional airfoil NACA 4415.

Methodology

Governing Equations

The governing equations of flow around an airfoil are the continuity equation, conservation of momentum, and the energy equation (ANSYS 2013). The equations are defined respectively as:

$$\frac{\partial \rho}{\partial t} + \frac{\partial}{\partial x_j}\left(\rho U_j\right) = 0 \quad (1)$$

$$\frac{\partial \rho U_i}{\partial t} + \frac{\partial \rho U_i U_j}{\partial x} = -\frac{\partial \rho}{\partial x_j} + \frac{\partial}{\partial x_i}\left(\mu \frac{\partial U_i}{\partial x_j} - \rho\overline{U_\iota U_J}\right) \quad (2)$$

$$\frac{\partial}{\partial x}(\rho E) + \nabla.\left(\vec{v}\,(\rho E + \rho)\right) = \nabla.\left(k_{eff}\,\nabla \mathrm{T}\right) + S_h \quad (3)$$

$\rho\overline{U_\iota U_J}$ is the turbulent Reynolds stresses as defined in linear eddy viscosity models as:

$$\overline{u_\iota u_J} = \frac{2}{3}k\delta_{ij} - \nu_t\left(\frac{\partial U_i}{\partial x_j} + \frac{\partial U_j}{\partial x_i}\right) \quad (4)$$

Here ν_t is the turbulent viscosity. ρ, E, T, k_{eff}, S_h, represents the density, energy, temperature, effective thermal conductivity, and the source term respectively.

Numerical modeling

The governing equations were discretized by the finite volume technique (Versteeg and Malalasekera 2007). The Spalart-Allmaras model is such a one-equation model that solves a modeled transport equation for the kinematic eddy (turbulent) viscosity (Spalart and Allmaras 1992). The Spalart-Allmaras model was formulated purposefully for applications in the field of aerospace where wall-bounded flows are significant and it has been shown to give good results for turbulence boundary layers subjected to adverse pressure gradients.

In its basic form, the Spalart-Allmaras model is essentially a low-Reynolds number model, requiring the viscosity-affected region of the boundary layer to be properly resolved for $y^+ \sim 1$ meshes (ANSYS 2013). The transported variable in the Spalart-Allmaras model $\tilde{\nu}$, is identical to the turbulent kinematic viscosity except in the near-wall (viscosity-affected) region. The transport equation for $\tilde{\nu}$ is:

$$\frac{\partial}{\partial t}(\rho\tilde{\nu}) + \frac{\partial}{\partial x_i}(\rho\tilde{\nu}u_i) = G_\nu + \frac{1}{\sigma_{\tilde{\nu}}}\left[\frac{\partial}{\partial x_j}\left\{(\mu + \rho\tilde{\nu})\frac{\partial \tilde{\nu}}{\partial x_j}\right\} + C_{b2\rho}(\frac{\partial \tilde{\nu}}{\partial x_j})^2\right] - Y_\nu + S_{\tilde{\nu}} \quad (5)$$

Here G_ν is the production of turbulent viscosity, and Y_ν is the destruction of turbulent viscosity that occurs in the near-wall region due to wall blocking and viscous damping. $\sigma_{\tilde{\nu}}$ and C_{b2} are the constants and are the molecular kinematic viscosity. $S_{\tilde{\nu}}$ is a user-defined source term. As the turbulence kinetic energy, κ is not calculated in the Spalart-Allmaras model, the last term in Equation (3) is ignored when estimating the Reynolds stresses (ANSYS 2013).

Finally, the general equations for the coefficients of drag, C_D and lift, C_L (Cengel and Cimbala 2013) are:

$$C_D = \frac{F_D}{\frac{1}{2}\rho V^2 A} \tag{6}$$

$$C_L = \frac{F_L}{\frac{1}{2}\rho V^2 A} \tag{7}$$

Here, V is the upstream velocity, A is the frontal area, F_D and F_L are the drag force and the lift force respectively.

Model Geometry and Meshing Technique

The geometry of this model is a 2D arrangement. Each of the four airfoil configurations was created and analyzed using a commercial programming bundle named ANSYS FLUENT. A rectangular-shaped space is defined as having a length to width ratio of 3:2 shown in Figure 3. National Advisory Committee for Aeronautics (NACA 4415) airfoil (Arthur 1971) was picked to contrast the outcomes of three types of KFm airfoils. For all the four airfoils, chord length was equivalent. Kline-Fogleman adjusted 1 (KFm-1) airfoil has around 7-9% thickness and its step was drawn at 40% of its chord length. But for the KFm-2 step was at 50% of its chord length. For KFm-3 airfoil, it has around 9-12% thickness and two steps are positioned at 50% and 75% of its chord length. After design parameters were set, the mesh was generated by ANSYS FLUENT default set up.

Figure 4 shows the meshing for four distinct airfoils. In the arrangement partition, the Solver type was picked as pressure based on an incompressible stream. Time was set as reliable and 2D space was picked as an organizer. Table 1 shows the residual convergence criterion. Reynolds number was 3.18×10^5 because airspeed was taken 5 ms^{-1}. The measured pressure was taken as zero and the weight outlet was given as barometrical weight. The atmospheric pressure was selected as 101,325 Pa. Finally, there was a no-slip condition applied around the solid surface.

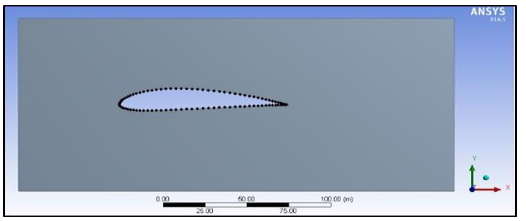

Figure 3: (a) Computational domain setup for NACA 4415

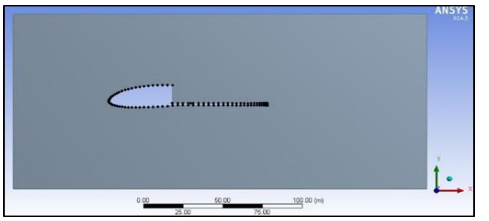

Figure 3: (b) Computational domain setup for KFm-1

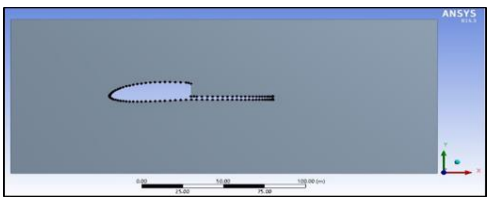

Figure 3: (c) Computational domain setup for KFm-2

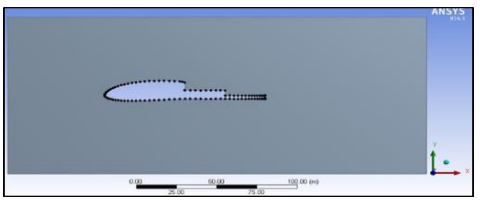

Figure 3: (d) Computational domain setup for KFm-3

Table 1: Residual convergence criterion for solution quantities

Variable	Continuity	u_x	u_y	Energy	Nut
Convergence Criterion	$\leq 10^{-3}$	$\leq 10^{-3}$	$\leq 10^{-3}$	$\leq 10^{-6}$	$\leq 10^{-3}$

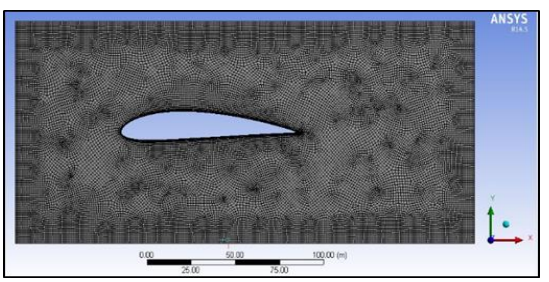

Figure 4: (a) Mesh diagram for NACA 4415

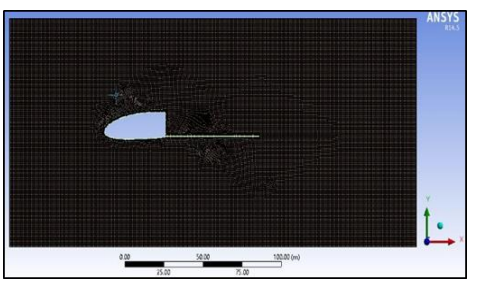

Figure 4: (b) Mesh diagram for KFm-1

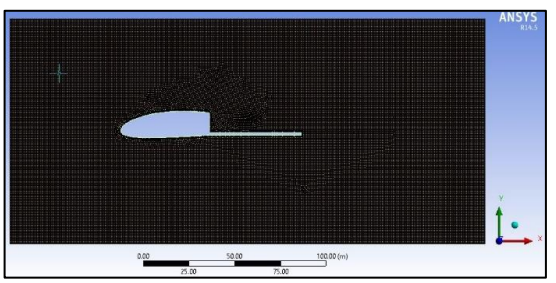

Figure 4: (c) Mesh diagram for KFm-2

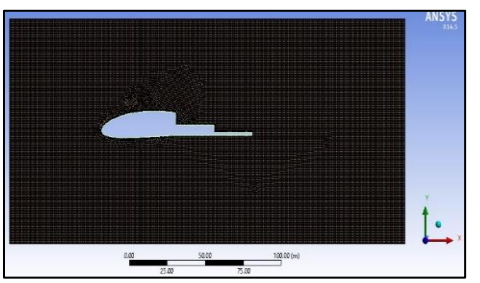

Figure 4: (d) Mesh diagram for KFm-3

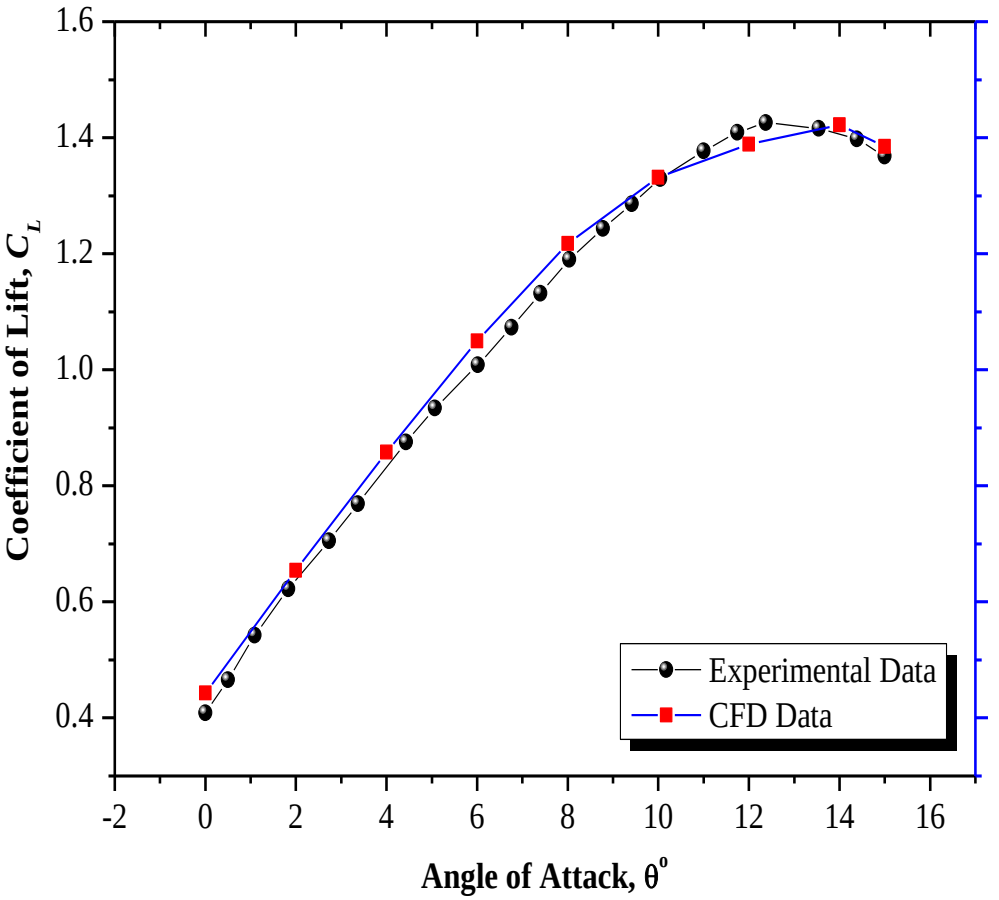

Figure 5: Validation of the simulation performance

Validation of the simulation

For the meshing and the subsequent simulation performance, validation was completed by comparing the experimental data of the coefficient of lift for NACA 4415 airfoil (Ranganadhan 2012) with the current simulated results of NACA 4415. The overall performance is generally agreeable as shown in Figure 5.

Results and Discussion

The impact of backward-facing steps on KFm Based Modified NACA 4415 airfoils is studied for better aerodynamic efficiency. The investigation is done for four distinct airfoils with four AOA (0˚, 5˚, 10˚, and 15˚) for a Mach number ranging from 0.3-0.6. The aerodynamic efficiency depends on the Coefficient of lift, $C_{L,}$ and coefficient of lift, C_D was measured for the different AOA. Figure 6 and 7, shows a comparison of these parameters for modified KFm airfoils.

It is evident from Figure 6 (a) that the coefficient of lift is highest for KFm-3 with a gentle slope for the four distinct AOA. But, the coefficient of drag shows little to almost no change (Figure 6 (b)) because of the position of the steps for KFm-1, KFm-2, or KFm-3 and only varies with AOA. Even though the coefficient of drag is independent of the backward step position for KFm airfoils, the overall aerodynamic efficiency is better for KFm-3 than the other two KFm airfoils due to its higher lift achieved by the two backward steps (Figure 7 a). Because of its better efficiency, KFm-3 is compared with the NACA 4415 airfoil for aerodynamic efficiency in Figure 7 (b).

It is pertinent from Figure 7 (b) that KFm-3 performs better than the traditional NACA airfoil at the same AOA. However, for both graphs, a sharp drop in aerodynamic efficiency is noted with respect to AOA since the drag coefficient increases as well. The increasing drag force introduces stalling to the airfoils and reduces its performance significantly.

Figure 8 compares the trailing vortices generated by the four airfoils at a constant AOA of 0° and 15^o with a Mach number of 0.3 and 0.6. The CFD images, from Figure 8, show that AOA of 0° the overall trailing vortices pattern remains similar for Mach number 0.3 and 0.6. However, for 0.6 MACH number all three KFm, KFm-1, 2, and 3, shows as the AOA increases, the trailing vortices display a distinct turbulent vortex shedding pattern. This indicates that, at higher AOA, the KFm airfoils start to show significant effects of stalling whereas NACA 4415 airfoil performs relatively well even at a high AOA of 15^o and Mach number. The comparison indicates with the introduction of backward-facing steps in KFm generates fluctuating trailing vortices which produces a lack of stability and reduces efficiency.

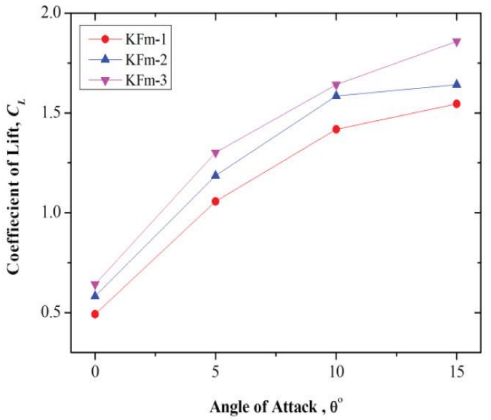

Figure 6: (a) C_L versus AOA

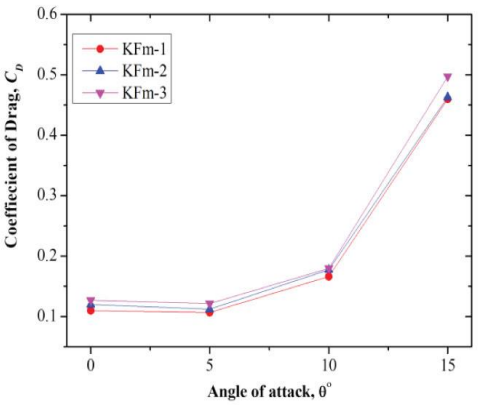

Figure 6: (b) C_D versus AOA

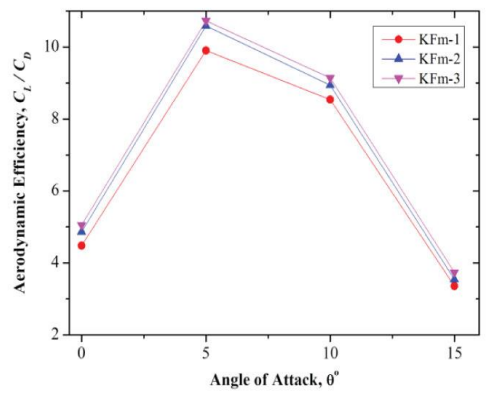

Figure 7: (a) Aerodynamic Efficiency versus AOAfor KFm airfoil series

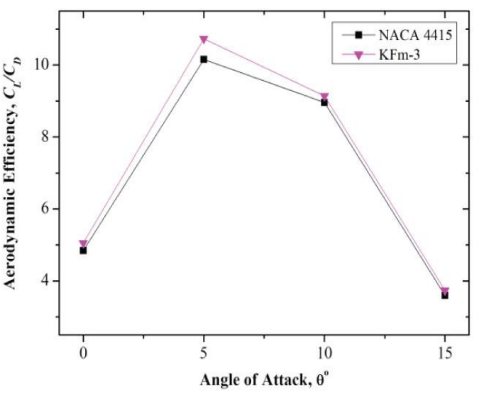

Figure 7: (b) Aerodynamic Efficiency comparison of NACA 4415 and KFm-3 airfoil for KFm airfoil series

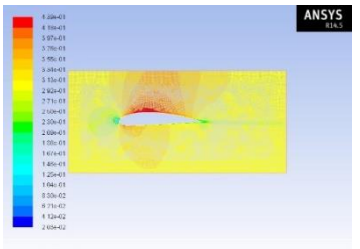

Figure 8: (a) NACA 4415 with AOA 0^{o} and Mach number 0.3

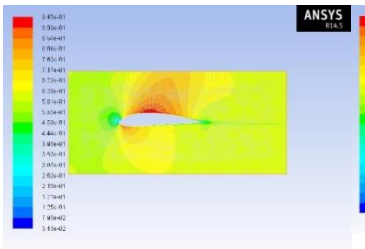

Figure 8: (b) NACA 4415 with AOA 0^{o} and Mach number 0.6

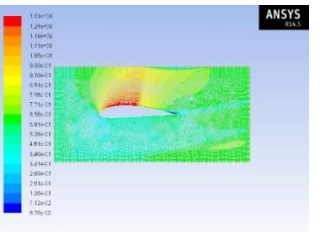

Figure 8: (c) NACA 4415 with AOA 15^{o} and Mach number 0.6

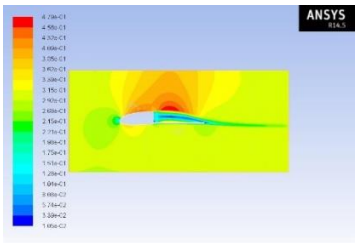

Figure 8: (d) KFm-1 with AOA 0^{o} and Mach number 0.3

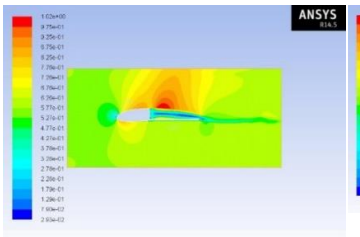

Figure 8: (e) KFm-1 with AOA 0^{o} and Mach number 0.6

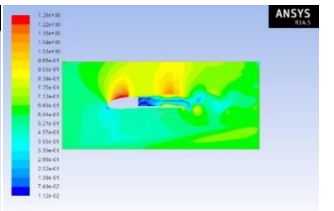

Figure 8: (f) KFm-1 with AOA 15^{o} and Mach number 0.6

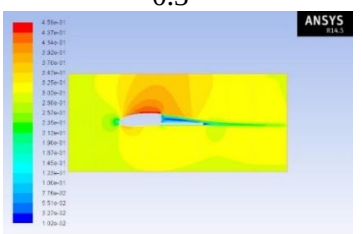

Figure 8: (g) KFm-2 with AOA 0^{o} and Mach number 0.3

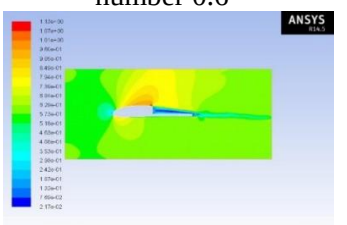

Figure 8: (h) KFm-2 with AOA 0^{o} and Mach number 0.6

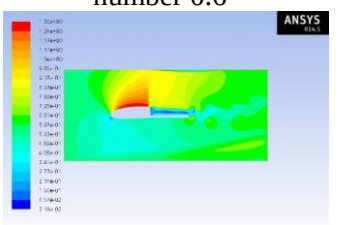

Figure 8: (i) KFm-2 with AOA 15^{o} and Mach number 0.6

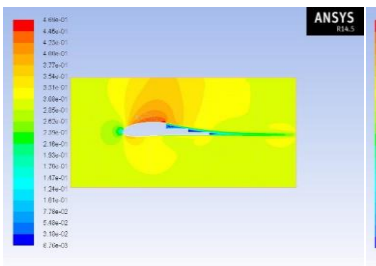

Figure 8: (j) KFm-3 with AOA 0^{o} and Mach number 0.3

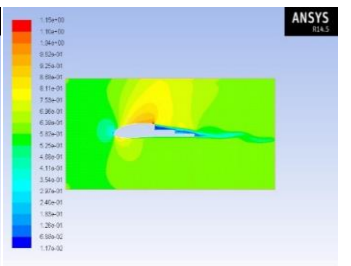

Figure 8: (k) KFm-3 with AOA 0^{o} and Mach number 0.6

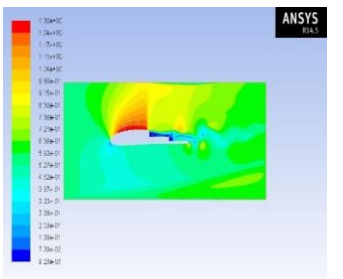

Figure 8: (l) KFm-3 with AOA 15^{o} and Mach number 0.6

These particular behaviors are the key factors behind KFm airfoils' limited application in the world of aerodynamics. As a result of this, the KFm series airfoil application is mostly limited to small scale low weight carrying aircrafts such as remote-controlled lightweight aircraft instead of commercial aircraft where their ability to generate lift force is highly sought after without investing a significant amount of effort or energy.

Conclusion

NACA airfoil series is described by the 4 digits which appoint the camber, position of the best camber, and thickness. In this research work, the aerodynamic performance of NACA 4415 and the KFm based three airfoils was measured and compared to highlight the importance of having a passive form of vortex generation with backward-facing steps. Based on the analyses that were carried out, several outcomes are noted.

KFm-1 airfoil is a good utility airfoil but it is superseded by the KFm-2. KFm-2 has a higher lift than KFm-1 so that its center of pressure is stable. Since the KFm-3 airfoil has a higher lift than the previous two KFm based airfoil, this airfoil can be used for slightly heavier lifting. Therefore, KFm-3 was the best performer of the three modified airfoils and its performance was better compared to the more traditional NACA series airfoil. KFm-3 with two backward-facing steps showed improved aerodynamic efficiency compared to the NACA 4415 airfoil. Since the Analysis was chosen to be carried out in a 2D format, the Spalart-Allmaras model naturally captured the lift and drag trends subsequently well. However, this model does not consider the turbulence kinetic energy, κ. As a result, future research may be carried out with other complex and versatile turbulence models such as k-ε, k-ω, low Reynolds number k-ε, SST k-ω, and v2-f turbulence models, etc. This may be able to get us a complete picture of various turbulence models' overall performance for numerically analyzing a variety of airfoil designs (such as KFm-4, 5, 6, etc.) along with detailed images of vortex shedding.

References

Abbott, Ira HA, and Albert E. Von Doenhoff. 2012. *Theory of wing sections: including a summary of airfoil data.* Courier Corporation.

ANSYS. 2013. "ANSYS Fluent Theory Guide." Canonsburg, Pa: ANSYS, Inc., November. *http://www.ansys.com.*

Arthur, Carter W. 1971. *Pressure Distributions On A Wing Having Naca 4415 Airfoil Sections With Trailing-Edge Flaps Set At 0^0 And 40^0*. Washington D.C.: National Aeronautics and Space Administration. https://ntrs.nasa.gov/archive/nasa/casi.ntrs.nasa.gov/19710018601.pdf

Asif, Kabir Mohammad, Mehran Islam, Yeasir Mohammad Akib, and Ahsan Hafiz. 2019. "Comparison between two Kline-Fogleman Modified (KFm) based Stepped Airfoils for better Aerodynamic Performance." *2nd International Conference on Innovation in Engineering and Technology (ICIET) 2019.* Dhaka: IEEE.

Bandakkanavar, Ravi. 2015. krazytech. February 10. https://krazytech.com/technical-papers/introduction-airfoil.

Boroomand, Masoud, and Shirzad Hosseinverdi. 2009. "Numerical investigation of turbulent flow around a stepped airfoil at high Reynolds number." *ASME 2009 fluids engineering division summer meeting.* American Society of Mechanical Engineers Digital Collection. 2163-2174.

Cengel, Yunus, and John Cimbala. 2013. Fluid Mechanics Fundamentals and Applications. 3rd. New York: McGraw-Hill Education.

Davereap. 2017. *FLITETEST.* April. Accessed March 2020. https://www.flitetest.com/articles/kfm-wings-a-basic-explanation.

Fertis, Demeter G. 1994. "New airfoil-design concept with improved aerodynamic characteristics." *Journal of Aerospace Engineering* 7 (3): 328-339.

Hasan, Mahdi, Asif Kabir, and Yeasir Mohammad Akib. 2019. "Dynamic Stall Investigation of Two Dimensional Vertical Axis Wind Turbine Blades Using Computational Fluid Dynamics." AIP Conference Proceedings. doi:https://doi.org/10.1063/1.5115940.

Kabir, A., M. Hasan, and Y. M. Akib. 2019. "Numerical Analysis on Naca0012 Airfoil at Different Mach Numbers with Varying Angle of Attacks Using Computational Fluid Dynamics." *International Conference on Engineering, Research, Innovation, and Education (ICERIE, 2019).* Sylhet.

Kabir, A., SM M. Hossain, A. Hafiz, and A. A. Sayeed. 2019. "Aerodynamic Analysis on Double Wedge Airfoil at Different Mach Numbers with Varying Angle of Attacks Using Computational Fluid Dynamics." *2019 International Conference on Computer, Communication, Chemical, Materials, and Electronics Engineering.* Rajshahi: IEEE. 1-6.

Kabir, Asif, Md Saadbin Chowdhury, Md Jahirul Islam, and Mehran Islam. 2019. "Numerical Assessment of the Backward Facing Step for NACA 0015 Airfoil using Computational Fluid Dynamics." *2019 1st International Conference on Advances in Science, Engineering, and Robotics Technology (ICASERT).* Dhaka: IEEE. 1-6.

Kabir, Asif, Yeasir Mohammad Akib, Ahsan Hafiz, and Avijit Mallik. 2019. "A Computational Design Approach on KFm Based Modified NACA-4415 for Better

Aerodynamic Efficiency." *2019 5th International Conference on Advances in Electrical Engineering (ICAEE).* Dhaka: IEEE. 468-472.

Kasper, Witold A. 1975. *Some Ideas of Vortex Lift.* Technical Paper, SAE.

Kline, Richard L., and Floyd F. Fogleman. 1977. Airfoil for aircraft having improved lift generating device. US Patent 4,046,338.

Kruppa, Edward W. 1977. "Wind-Tunnel Investigation Of Kasper Vortex Concept." *Astronautics & Aeronautics* (American Institute of Aeronautics and Astronautics) 15 (10): B10-B10.

Ranganadhan, Voona. 2012. *Enhancing the aerodynamic performance of stepped airfoils.* Masters Theses, Rolla: Missouri University of Science and Technology. https://scholarsmine.mst.edu/masters_theses/6897.

Spalart, Philippe, and Steven Allmaras. 1992. "A one-equation turbulence model for aerodynamic flows." *30th Aerospace Sciences Meeting and Exhibit.* Reno: American Institute of Aeronautics and Astronautics. doi:https://doi.org/10.2514/6.1992-439.

Versteeg, Henk Kaarle, and Weeratunge Malalasekera. 2007. *An Introduction to Computational Fluid Dynamics: The Finite Volume Method.* Pearson education.

Witherspoon, Stephen, and Fathi Finaish. 1996. "Experimental and Computational studies of flow developments around an airfoil with backward-facing steps." *14th Applied Aerodynamics Conference.* American Institute of Aeronautics and Astronautics. 2481.